

How to compute using globally coupled oscillators

Peter Ashwin and Jon Borresen

*Department of Mathematical Sciences,
University of Exeter, Exeter EX4 4QE, UK*

(Dated: November 15, 2018)

Abstract

Synchronization is known to play a vital role within many highly connected neural systems such as the olfactory systems of fish and insects. In this paper we show how one can robustly and effectively perform practical computations using small perturbations to a very simple globally coupled network of coupled oscillators. Computations are performed by exploiting the spatio-temporal dynamics of a robust attracting heteroclinic network (also referred to as ‘winnerless competition’ dynamics). We use different cluster synchronization states to encode memory states and use this to design a simple multi-base counter. The simulations indicate that this gives a robust computational system exploiting the natural dynamics of the system.

PACS numbers: 05.45, 87.10.+e

Recent experimental and theoretical work by several authors has highlighted the crucial role of spatio-temporal dynamics in neural systems. In particular, work on olfactory systems of insects and fish has demonstrated that recognized odors manifest themselves as different spatio-temporal outputs from certain sub-systems such as [1, 2, 3, 4] for insect antennal lobes (AL) and [5, 6] for the Zebrafish olfactory bulb (OB). It has been suggested that the dynamics of the network responsible for the transformation of input to output of the AL/OB for these systems is one of ‘winnerless competition’ [7, 8, 9]; this is a class of attracting dynamics consisting of saddle periodic orbits linked together by unstable manifolds. Such attractors may seem at first unnatural but in systems that are close to symmetric and in systems that have invariant subspaces they may be robust; i.e. they may persist under arbitrary perturbations that preserve the symmetric (or invariant subspace) structure. Such attractors have been found in a range of physically relevant models and experiments [10, 11].

The AL/OB system is far from being a simple relay; it shows effects such as short term memory, anticipation and computation [7]. The aim of this paper is to show that globally coupled systems idealizing the AL/OB architecture can be used to explicitly design computational systems by exploiting robust heteroclinic attractors (winnerless competition). We use globally coupled phase oscillators in regimes where one finds slow switching between cluster states [12, 13, 14, 15]. Previous work has shown [16] that robust heteroclinic attractors for a particular system of five globally coupled phase oscillators allow one to encode up to twenty different memory states as synchronized clusters, and moreover to effectively move between them by means of small perturbations. The number of such states scales exponentially with N the number of oscillators. In this paper we go further to show that one can in principle perform arbitrary computations using a globally coupled cluster for ‘memory/timing’ on addition of perturbations that may have very low amplitude.

We consider perturbations to the model of Hansel *et al.* [12] for N globally coupled oscillators with phases $\theta_i \in \mathbf{T} = [0, 2\pi)$ given by

$$\dot{\theta}_i = \omega + \frac{1}{N} \sum_{j=1}^N g(\theta_i - \theta_j) + \eta w_i(t) + \epsilon I_i(t), \quad (1)$$

when $i = 1, \dots, N$ and $g(\phi) = -\sin(\phi + \alpha) + r \sin(2\phi)$; see also [13, 14, 15]. The quantities $w_i(t)$ represent derivatives of independent, identically distributed Brownian processes with zero mean and unit variance per unit time. The inputs $|I_i(t)| \leq 1$ are used to control the state of the system. We include η and ϵ , small parameters that control the strength of the

noise and perturbations respectively.

The system (1) for the unperturbed system ($\eta = \epsilon = 0$) has symmetry \mathbf{S}_N corresponding to permutations of the N oscillators. Using these symmetries one can identify robust heteroclinic attractors (first noted theoretically in [11] and then practically for this example in [12]) that exist for open sets of parameters. For certain parameter values the attractors consist of saddle periodic orbits of symmetry $\mathbf{S}_k \times \mathbf{S}_{N-k}$, i.e. states where all oscillators are in one of two possible phases at any point in time and such that precisely k of them are in one phase. The system also has an \mathbf{S}^1 phase-shift symmetry that allows one to characterize periodic orbits as group orbits. For

$$N = 5, \alpha = 1.25, \omega = 5, r = 0.25, \quad (2)$$

the only attractor for unperturbed (1) consists of twenty periodic orbits with symmetry $\mathbf{S}_2 \times \mathbf{S}_3$ and their unstable invariant manifolds. This forms them into a single strongly connected network.

The periodic orbits involved are \mathbf{S}^1 orbits of $x_j = (0, 0, 0, \psi_j, \psi_j)$ with $j = 1, 2$ and permutations thereof. We list a set of permutations σ_k with $k = 1, \dots, 10$ that map the periodic orbit through x_j onto the 10 possible symmetric images and denote by P_j^k the periodic orbit given by the \mathbf{S}^1 orbit of $\sigma_k x_j$ for $j = 1, 2$ and $k = 1, \dots, 10$. These periodic orbits are listed in Table I. For the given parameters (2), $\psi_1 = 1.339$ and $\psi_2 = 0.799$ [16]. If we write $\Sigma = \bigcup_{i=1}^{10} \bigcup_{j=1}^2 W^u(P_j^k)$ where $W^u(P)$ is the unstable manifold of the saddle periodic orbit P then any randomly chosen initial condition approaches Σ ; this manifests itself as a sequence of ‘slowing down’ switchings between different cluster states P_j^k . Figure 1 shows a detail of the unstable manifold of one of the P_1^k .

For larger N (1) displays heteroclinic cycles between $\mathbf{S}_k \times \mathbf{S}_{N-k}$ symmetry states for a variety of k with $N/3 < k \leq N/2$ [14]; this gives rise to more complicated attracting heteroclinic networks that are currently under investigation by the authors. The unperturbed dynamics is such that after a transient period the system state is near one of the P_j^k except for increasingly occasional short transitions. As Σ is asymptotically stable this is also true even for the perturbed system as long as the perturbation is small enough. We exploit this feature for our computational system. Typical initial conditions for the unperturbed system lead to an asymptotic state that is a slowing-down oscillation between P_1^k and P_2^k for some k determined by the initial condition.

Trajectories of the perturbed system may visit many or all P_j^k where j always alternates between 1 and 2 and k changes on a longer timescale [16]. This is because the unstable manifold of P_1^k is two dimensional and only exceptional trajectories on this connect to P_2^l with $k \neq l$. In the presence of noise we refer to the average time of switching between P_j^k as the *cycling time* T_c ; one can show that this scales as $-\ln \eta$ [12]. The average time of switching between P_j^k with different k we refer to as the *switching time* T_s . The order parameter $\chi = \frac{1}{N} \left| \sum_{k=1}^N e^{i\theta_k} \right|$ often considered for such systems [12, 14] oscillates at a rate given by the cycling time. Because this measure is invariant under permutations of the phases it is not possible to detect switches and compute T_s using only χ .

One can view the globally coupled system (1) as a computational system with five inputs $I_i(t)$, $i = 1..5$ and twenty outputs $Y_j^k(\theta) = |\theta - P_j^k|_1$ (where $|\theta|_1 = \sum_i |\theta_i|$), namely if Y_j^k is small then the trajectory is close to P_j^k . Figure 2 shows the statistics of δ , the local minimum of the Y_j^k over one cycle. The mean $\langle \delta \rangle$ varies proportionally as the square root of the noise, reminiscent of the algebraic scaling in heteroclinic switching rates with noise level found in [17]. Defining the mean probability of switching per cycle P_s , we can estimate $P_s = T_c/T_s$. Numerical simulations indicate that $T_s/T_c = O(\eta^{1/2})$ as $\eta \rightarrow 0$; see Figure 3, where we detect close approaches by $|\theta - P_j^k|_1 < \Delta$ where $\Delta = 10\sqrt{\epsilon}$. This ensures that all the switches found in Figure 2 are registered while it avoids false positive detections of switching, as (for instance) may occur on a trajectories moving between P_1^1 and P_2^1 passing very close to P_2^9 or P_2^2 (see Figure (1)). One can then use simple logic gates to connect up outputs and inputs to form a computational system.

As a proof-of-principal, we have used (1) to construct a counter that counts in either base 5 or base 2 depending on initial condition to the phases. The inputs we consider are $C(t)$ a clock pulse that occurs at approximately regular intervals and $X(t)$ an input that may or may not occur between clock pulses. We construct the system so that pulses of $C(t)$ occurring at a state P_2^k perturb the system along the unstable manifold towards P_1^k and pulses of $X(t)$ occurring at a state P_1^k perturb the system along the unstable manifold towards $P_1^{\ell(k)}$ where $\ell = [1, 3, 4, 5, 6, 2, 8, 7, 9, 10]$. In each case this corresponds to simply applying a pulse to input $I_{p(k)}$ where $p = [4, 4, 1, 3, 2, 5, 3, 3, 2, 1]$. In this way we effectively define functions $I_i = F_1(Y_j^k)X + F_2(Y_j^k)C$ that steer the state of the system around the network rapidly and reliably even when ϵ is very small, depending on the inputs X and C . We show the setup schematically in Figure 4; Figure 5 shows the counter functioning accurately for an initial

condition near P_1^2 . Figure 6 shows simulations on changing parameters and in the last case, initial conditions.

There is a trade-off between on the one hand the speed of computation and on the other hand its accuracy and sensitivity to noise. In particular the input amplitude ϵ gives a characteristic cycle time as does the noise amplitude η . For effective computation in the above system we need $1 \gg \epsilon \gg \eta$ and the clock cycles must lie between the cycle times associated to the two perturbation amplitudes.

Many models use oscillators to perform computational tasks, for example [19]. The novelty in this work is that we demonstrate how one of the simplest possible types of coupling can give rise to robust attracting heteroclinic networks that one can exploit to perform computations. As in winnerless competition models [1, 8, 9] the average phase differences in the globally coupled system change very little depending on the state of the system and the computation is performed by following natural trajectories within the system. Moreover, the state of the system is not detectable from individual or ‘mean’ cell outputs but is encoded globally. By contrast, if we use asymptotically stable attractors for storing memory states comparatively large perturbations to the system will be needed to lift it out of the basin of attraction into another state.

The mechanism we consider is a winnerless competition model using (a) two dimensional manifolds which allow many possibilities to be considered at each state and so allows the network to scale to large numbers of states without greatly increasing the average length of path (b) the dynamics requires no careful tuning for a range of coupling parameters, nor plasticity in the coupling. We use two populations of processing elements (a) the globally coupled oscillators θ_i have the function of a ‘memory/timing’ circuit and (b) observables Y_j^k from the system that detect presence of a particular cluster state. The latter are analogous to certain Kenyon Cells in the mushroom body that receive inputs from an insect antennal lobe [3, 4, 7, 18] and decode a large dense set of states in a relatively low dimensional space to a sparse set of states in a higher dimensional space.

We believe that the simple global coupling used within the ‘processing element’ of our model is a positive feature. Although symmetry is never achieved, the observation that the heteroclinic attractor is asymptotically stable means that the dynamics are well modelled even when global coupling is perturbed. There may be evolutionary advantages to having neural subsystems that attempt to approach symmetric coupling as this can presumably

be encoded genetically very simply (see [20] for other approaches to neural information processing that use symmetries). The fact that the dynamics of the unperturbed system is robust means that heteroclinic attractors are model-independent and will exist in globally coupled systems of phase oscillators [11, 21], coupled ODE oscillators or even piecewise smooth systems of phase-resetting oscillators [22].

The dynamics we use is not present in $N \leq 4$ oscillators; to find robust heteroclinic attractors with unstable manifolds of higher than one dimension we need $N \geq 5$ [16]. The ideas presented should scale well on increasing N beyond 5; the number of cluster states grows exponentially but the diameter of the heteroclinic network need not grow, meaning that rapid transition from one state to another is still possible. Note we do not claim that any particular AL/OB neural system functions via perturbations to a robust heteroclinic attractor (though this has been suggested [1]). We do show that a globally coupled system of phase oscillators allows rapid and reliable computation.

Acknowledgments: We acknowledge very interesting discussions with Roman Borisyuk, David Corne, Gerhard Dangelmayr and Marc Timme concerning this research. The research of JB is supported by an EPSRC studentship and that of PA by a Leverhulme research fellowship. We are very grateful for the hospitality and financial support of the MPI für Strömungsforschung, Göttingen.

-
- [1] M. Rabinovich, A. Volkovskii, P. Lecanda, R. Huerta, H. Abarbanel and G. Laurent, *Phys. Rev. Lett.* **87**, 068102 (2001).
 - [2] G.B. Burg, C.G. Galizia, R. Brandt and H. Mustaparta, *J. Comp. Neurology* **446**, 123–134 (2002).
 - [3] D. Martinez and E. Hugues. *Proc. NATO ARW, Oct 1-2 2003, Coventry 2003* (2003).
 - [4] R. Huerta, T. Nowotny, M.G. Sanchez, H.D.I. Abarbanel and M.I. Rabinovich, *Neural Computation* **16**, 1601–1604 (2004).
 - [5] R.W. Friedrich and G. Laurent, *J. Neurophysiol.* **91**, 2658–2669 (2004).
 - [6] R.W. Friedrich, C.J. Habermann and G. Laurent, *Nature Neuroscience* **7**, 862–871 (2004).
 - [7] G. Laurent, M. Stopfer, R.W. Friedrich, M.I. Rabinovich, A. Volkovskii and H.D.I. Abarbanel, *Ann. Rev. Neurosci.* **24**, 263–297 (2001).

- [8] V. Aframovich, M. Rabinovich and P. Varona, *Int. J. Bifurcation and Chaos* **14**, 4 (2004).
- [9] P. Seliger, L. Tsimring and M. Rabinovich, *Phys. Rev. E* **67**, 011905 (2003).
- [10] M. Krupa, *J. of Nonlinear Sci.* **7**, 129-176 (1997).
- [11] P. Ashwin and J.W. Swift, *J. Nonlinear Sci.* **2**, 69–108 (1992); P. Ashwin and P. Chossat, *J. Nonlin. Sci.* **8**, 103–129 (1998); P. Ashwin and M. Field, *Arch. Rational Mech. Anal.* **148**, 107–143 (1999).
- [12] D. Hansel, G. Mato and C. Meunier, *Phys. Rev. E* **48**, 3470–3477 (1993).
- [13] D. Hansel, G. Mato and C. Meunier, *Europhys. Letts.* **23**, 367–372 (1993).
- [14] H. Kori and Y. Kuramoto, *Phys. Rev. E* **63**, 046214 (2001).
- [15] H. Kori, *Phys. Rev. E* **68**, 021919 (2003).
- [16] P. Ashwin and J. Borresen, *Phys. Rev. E* **70**, 026203 (2004).
- [17] D. Armbruster, E. Stone and V. Kirk, *Chaos* **13**, 71–79 (2003).
- [18] O. Perez-Orive, J. Mazor, G.C. Turner, S. Cassanaer, R.I. Wilson and G. Laurent, *Science* **297**, 359–365 (2002).
- [19] R. Borisjuk, M. Denham, F. Hoppensteadt, Y. Kazanovich and O. Vinogradova, *Network: Comp. Neural Syst.* **12**, 1–20 (2001).
- [20] M. Breakspear, *Int. J. of Neural Systems* **11**, 101–124 (2001); D.L. Rowe, *Behavioural and Brain Sciences* **24**, 827–828 (2001); M. Breakspear, J.R. Terry and K.J. Friston. *Network: computation in Neural Systems* **14**, 703–732 (2003).
- [21] F.C. Hoppensteadt and E. Izhikevich, *Weakly Connected Neural Networks* Springer (2000).
- [22] M. Timme, F. Wolf and T. Geisel, *Phys. Rev. Lett.* **89**, 154105 (2002).

k	P_j^k	$\overline{W^u(P_1^k)} \supset$
1	$(0, 0, 0, \psi_j, \psi_j)$	P_2^2, P_2^9, P_2^{10}
2	$(\psi_j, \psi_j, 0, 0, 0)$	P_2^1, P_2^3, P_2^6
3	$(0, 0, \psi_j, 0, \psi_j)$	P_2^2, P_2^4, P_2^8
4	$(0, \psi_j, 0, \psi_j, 0)$	P_2^3, P_2^5, P_2^{10}
5	$(\psi_j, 0, 0, 0, \psi_j)$	P_2^4, P_2^6, P_2^9
6	$(0, 0, \psi_j, \psi_j, 0)$	P_2^2, P_2^5, P_2^7
7	$(0, \psi_j, 0, 0, \psi_j)$	P_2^6, P_2^8, P_2^{10}
8	$(\psi_j, 0, 0, \psi_j, 0)$	P_2^3, P_2^7, P_2^9
9	$(0, \psi_j, \psi_j, 0, 0)$	P_2^1, P_2^5, P_2^8
10	$(\psi_j, 0, \psi_j, 0, 0)$	P_2^1, P_2^4, P_2^7

TABLE I: Representative points on the periodic orbits P_j^k ($j = 1, 2, k = 1, \dots, 10$) in the unperturbed heteroclinic network (1); parameters as in (2). In all cases $\overline{W^u(P_j^k)} \supset P_{3-j}^k$, while $\overline{W^u(P_1^k)}$ contains the addition points listed (\overline{A} denotes the closure of the set A).

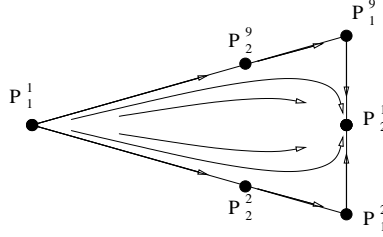


FIG. 1: Schematic showing part of the two dimensional unstable manifold $W^u(P_1^1)$; almost all trajectories leaving from P_1^1 converge to P_2^1 but exceptional trajectories converge to P_2^l for three possible $l \neq 1$, two of which are shown here.

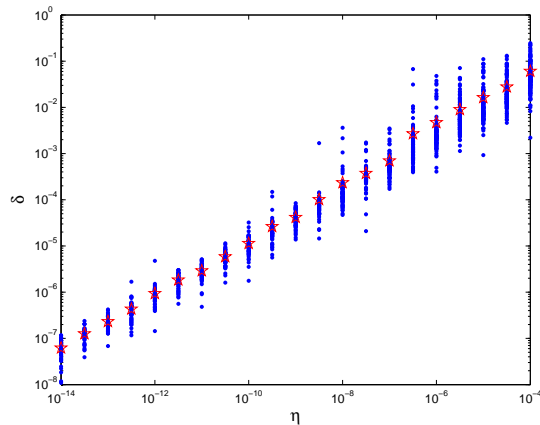


FIG. 2: Dots show the value of $\delta = \inf\{Y_j^k(t) : k, j, t \in [t_0, t_0 + T_c]\}$, the smallest value of any Y_j^k during a cycle time T_c in the presence of noise with amplitude η , after transients have decayed and for a range of random initial conditions. The mean closest approach (taking 100 cycles) scales as $\langle \delta \rangle = O(\sqrt{\eta})$.

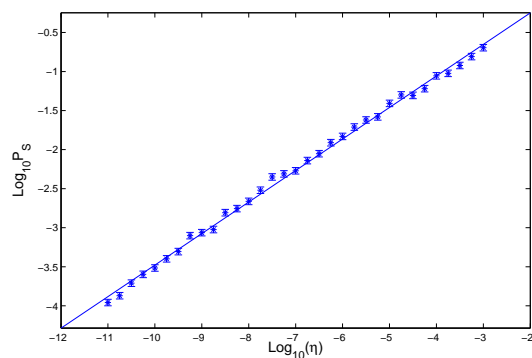


FIG. 3: Probability of switching P_s at each cycle for specified η with average over 100 trials. Error bars show two standard deviations and a least squares fit line is also included. This fits $P_s \sim \sqrt{\eta}$.

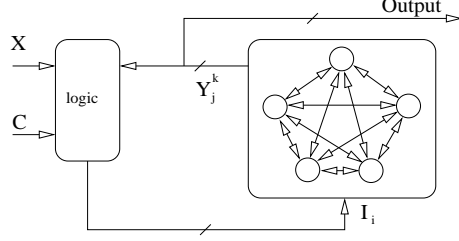


FIG. 4: Schematic wiring diagram for using the five-oscillator system for finite-state computation. The logic circuit steers the states around two possible periodic sequences of P_j^k depending on initial condition. The input to the system X and clock C are connected to one of the I_i depending only on which of the Y_j^k is lowest.

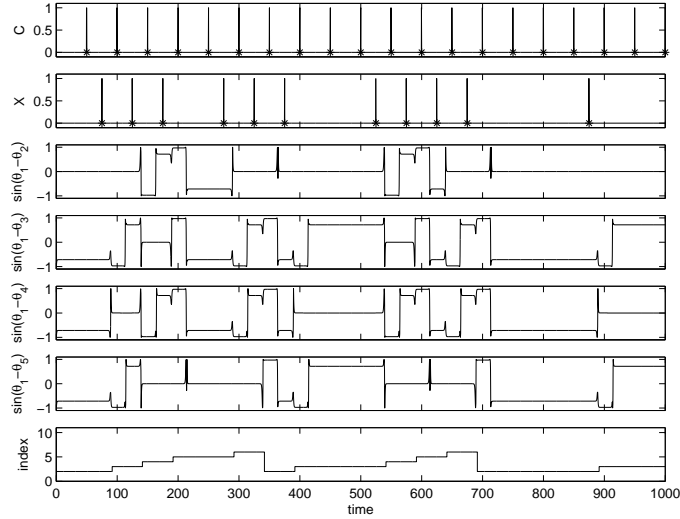


FIG. 5: Simulation of the counter for $C(t)$ and $X(t)$ as shown in the top graphs, for $\eta = 10^{-14}$ and $\epsilon = 10^{-10}$. The oscillator phase differences $\sin(\theta_1 - \theta_j)$ are shown, and the state index (bottom graph) cycles one step through states P_1^k where $k \in \{2, 3, 4, 5, 6\}$ each time an input on X is received. The same output is obtained robustly for a range of parameters.

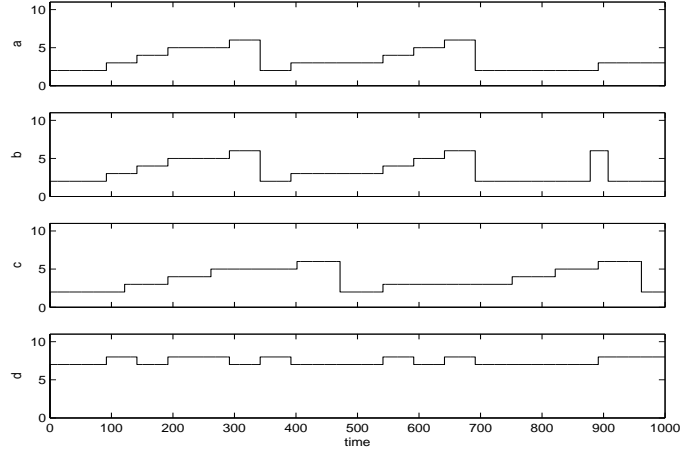


FIG. 6: Index giving the state of the counter for (a) the same inputs and initial condition as Figure 5; (b) as for (a) but increased η (observe the appearance of an erroneous switch just before $t = 900$); (c) as for (a) also reliably functions with the clock rate slowed from 50 to 70 time units; (d) as for (a) but starting with an initial condition near state 7; this shows the presence of a second cycle in the network.